Original Article

e-ISSN: 2775-5037
p-ISSN: 2614-3917

Original Article

Strengthening of Square Configuration Micropiles for Shallow Foundations Under Eccentric Loading on Soft Clay

Ahmad Dzikrullah Akbar[1]✉, Yudhi Lastiasih[2]
[1,2]Department of Civil Engineering, Faculty of Civil, Planning, and Earth Engineering, Institut Teknologi Sepuluh Nopember, Surabaya, Jawa Timur, Indonesia.
Correspondence Author: dzikrullhahakbar2@gmail.com✉

Abstract:

Soft clay soils pose a risk of sudden shear failure in shallow foundations, particularly under eccentric loading. This study examines the effectiveness of foundation reinforcement using square configuration micropiles to enhance bearing capacity under eccentric conditions. Numerical analysis was conducted using 2D plane strain modeling with the finite element method (Plaxis 2D) and the Soft Soil material model for cohesive clay with a shear strength of 14.85 kPa. Eccentricity variations (e/B = 0–0.25) were applied to evaluate changes in bearing capacity before and after reinforcement. The simulation results indicate that eccentricity reduces the foundation's bearing capacity by up to 44% compared to concentric loading. The installation of square micropiles increased the average bearing capacity by 51.47% compared to the unreinforced condition. Regression analysis resulted in an empirical equation for the increase in bearing capacity (Rq) influenced by the micropile's frictional resistance (Qs) and the composite system stiffness (Pmaks). These findings provide a practical design basis for shallow foundations in soft soils subjected to eccentric loads, thus enhancing the stability and safety of the structure.

Keywords: Numerical Analysis, Eccentric Load, Shallow Foundation, Soft Clay, Micropiles.

Submited : 14 Desember 2026
Revised : 5 Januari 2026
Acceptance : 12 Januari 2026
Publish Online : 15 Januari 2026

Introduction

The presence of thick soft clay soil presents a challenge in the design of shallow foundations. Foundations in such conditions are susceptible to sudden local shear failure due to the undrained behavior of the clay. Under undrained conditions, the shear strength of the clay is governed by undrained cohesion (cu), as the internal friction angle is zero (ϕu = 0). Studies using the assumption of vertical concentric loading have been conducted to evaluate the shear failure mechanism of soil under various shear strength conditions (Terzaghi, 1943). Based on these studies, soft clay typically undergoes local failure. The low shear strength results in maximum resisting stress (bearing capacity) that progresses to residual stress. However, the assumption

of vertical concentric loading is not applicable to the structural system's heterogeneity or the lateral loads often encountered in the field (R. Prakash & Rahul, 2020; Wang et al., 2021). Structural system heterogeneity in the field leads to variations in stress distribution and stress concentration due to the eccentricity of the load. Eccentric loading on a shallow foundation causes a reduction in bearing capacity and asymmetric deformation compared to concentric loading (Eastwood, 1955; Meyerhof, 1953; Michalowski & You, 1998; Okamura et al., 2002; S. Prakash & Saran, 1971; Purkayastha & Char, 1977).

Based on these challenges, the installation of micropiles cutting through the failure plane is proposed to increase the foundation's bearing capacity on soft clay and to limit lateral deformation. Although the length of the micropiles is limited in thick clay cases, micropile reinforcement provides a practical and cost-effective solution for simple structures such as steel warehouses, shop houses, and others. Previous studies using the assumption of vertical concentric loading showed that the use of micropiles effectively increased the bearing capacity (qult) of shallow foundations by 200% - 300% due to the shear strength increase resulting from micropile reinforcement cutting through the failure plane (Isnaniati & Mochtar, 2023). Laboratory studies, ranging from small to large scale, on concentric loading cases (Suroso et al., 2010, 2012; Tjandrawibawa, 2000; Tsukada et al., 2006) showed that bearing capacity improvements correlated with micropile geometry variables such as number, configuration, length, and diameter.

The effect of eccentric loading, which has not been previously addressed, may lead to a reduction in the effective vertical bearing capacity of piles due to the increase in eccentricity, as part of the pile's capacity is used to resist additional moments and shear forces (Dhana Sree et al., 2022; Franza & Sheil, 2021). Eccentric loading causes a dramatic change in the stress distribution around a single pile, with soil pressure becoming highly uneven, exhibiting high stress concentration on the side experiencing extreme compression due to the moment and potential stress reduction (or even gapping) on the opposite side (Seongcheol et al., 2021).

Considering this, the Micro Pile Raft (MPR) system is inherently more resistant to moments through the interaction of a distributed pile group, thus overcoming the problem of eccentricity compared to a single micropile (Alnuaim et al., 2016). The design of connected micropiles with the MPR system, with a limited number of micropiles, may lead to unreliable reinforcement due to large bending moments on each single pile at locations with high maximum axial stress concentration. Therefore, the application of unconnected piles and the addition of a compacted soil layer between the foundation and micropiles (Figure 1) is necessary to ensure the safety of the MPR system, even if the number of installed micropiles in the stress concentration area due to eccentric loading is limited. The investigation results of unconnected piles show good performance, reducing soil settlement by 35.6% and reducing shear load on the piles by 20.9% (Alhassani & Aljorany, 2019).

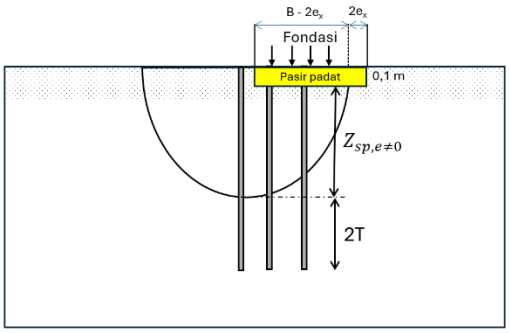

Figure 1. Schematic illustration of the unconnected micropile system under eccentric load.

In this study, the proposed micropile configuration is a square configuration that considers the effects of eccentric loading. Based on this configuration, numerical analysis with plane strain modeling using the 2D finite element method was employed to evaluate the bearing capacity of the foundation before and after being reinforced with micropiles on soft clay. The soft clay material, with a cohesion of 14.85 kPa, was modeled using the Soft Soil (SS) material model due to its simple shear strength and stiffness input parameters. The plane strain approach in this study results in continuous elongation behavior of the micropile model, thus assuming the behavior of the micropile and the soil between the micropiles as a composite material. The modeling analysis results were formulated with a ratio (Rq) approach between the bearing capacity of the foundation before and after reinforcement with the square-configured micropiles. The Rq value for each square configuration leads to an empirical equation determined by the micropile's end resistance (Qp), frictional resistance (Qs), and the micropile's stiffness (Pmaks) within the composite system. Considering the effect of eccentric loading that may occur in functional infrastructure built on very soft to soft soil, this research is essential to ensure that micropile reinforcement makes foundation systems safe, even under eccentric loads.

Methods

Sub 1 Model Material dan Parameter Tanah

The Soft Soil (SS) model is widely used for evaluating foundation problems (Agraine et al., 2020; Ambassa & Amba, 2020; Doherty et al., 2012; Li et al., 2025; Mohd et al., 2018; Waheed & Asmael, 2024; Waheed & Rahil, 2022). This model is developed from the Modified Cam Clay model and involves stiffness behavior determined by the nonlinear (logarithmic) relationship between the average effective stress (p') and volumetric strain (εv%), without considering the void ratio (e) (Brinkgreve, 2012). Meanwhile, the Mohr-Coulomb failure criterion is incorporated into the SS model to evaluate the soil's failure boundaries, as shown in Figure 2. Based on the failure boundaries in Figure 2, the formulation of the failure criterion is determined by Equation 1. The yield surface boundary is governed by the closed-form equation in Equation 2.

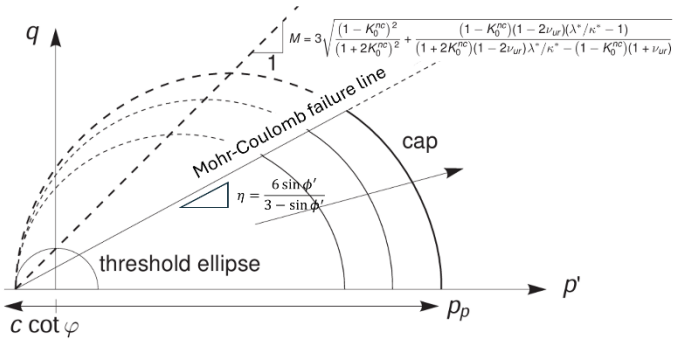

Figure 2. Failure Boundary and Yield Surface for the SS Model, modified from (Plaxis 2D 2025.1, 2025)

$$q = \frac{6\sin\phi'}{3-\sin\phi'}(p' + c'\cot\phi') \quad (1)$$

$$p' = p'_p - \frac{q^2}{M^2(p' + c'\cot\phi')} \quad (2)$$

Considering the stiffness behavior shown in Figure 3, the soil stiffness model is determined by the modified reloading gradient parameter (λ*) and the modified unloading gradient parameter (κ*). In the case of isotropic compression loading at the normal consolidated soil condition (OCR = 1), the relationship between volumetric strain change and the applied load is presented in Equation 3. Meanwhile, the formulation for the change in volumetric strain and the applied load under unloading conditions is presented in Equation 4.

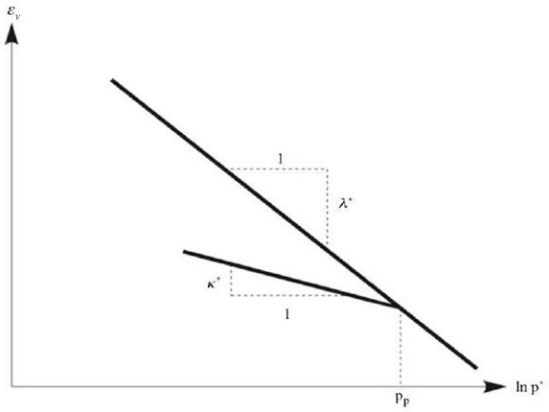

Figure 3. Relationship Curve of Volumetric Strain and Average Effective Stress (Plaxis 2D 2025.1, 2025).

$$\Delta\varepsilon_v = -\lambda^* \ln\left(\frac{p' + c'\cot\phi'}{p_0 + c'\cot\phi'}\right) \quad (3)$$

$$\Delta\varepsilon_v = -\kappa^* \ln\left(\frac{p' + c'\cot\phi'}{p_0 + c'\cot\phi'}\right) \quad (4)$$

Considering the undrained drainage type A behavior adopted in the SS model,

it is necessary to adjust the stiffness parameters and effective shear strength to produce a model behavior that can accommodate undrained conditions. Undrained conditions (c = cu, ϕ = ϕu = 0) can be accommodated when the ratio values of λ* and κ* are equal to 1. Therefore, the parameter data used in this study for soft clay soil is presented in Table 1. In addition, the soil is assumed to meet the normal consolidated soil condition (OCR = 1), with the soil stratification considered homogeneous, so the shear strength generated will remain constant with respect to soil depth.

Table 1. Soft Clay Soil Parameters for the SS Model Under Undrained Conditions

Parameter	Parameter Value
λ*	0,07671
κ*	0,076708661
K_o^{NC}	0,999982547
M	3,49 x 10^{-5}
υ'_{ur}	0,15
c' (kN/m²)	14,850
ϕ' (derajat)	0,001
γ_{sat} (kN/m³)	16,3

Sub 2 Shallow Foundation Modeling and Square Configuration Micropile

A 2D numerical analysis using Plaxis 2D v20 software was chosen to evaluate the bearing capacity of the foundation before and after reinforcement with micropiles on soft clay under eccentric loading (Figure 5(c)). The eccentricity variations applied in the modeling are 0, 0.1, 0.17, and 0.25. The flowchart for modeling the shallow foundation with and without micropiles is presented in Figure 4.

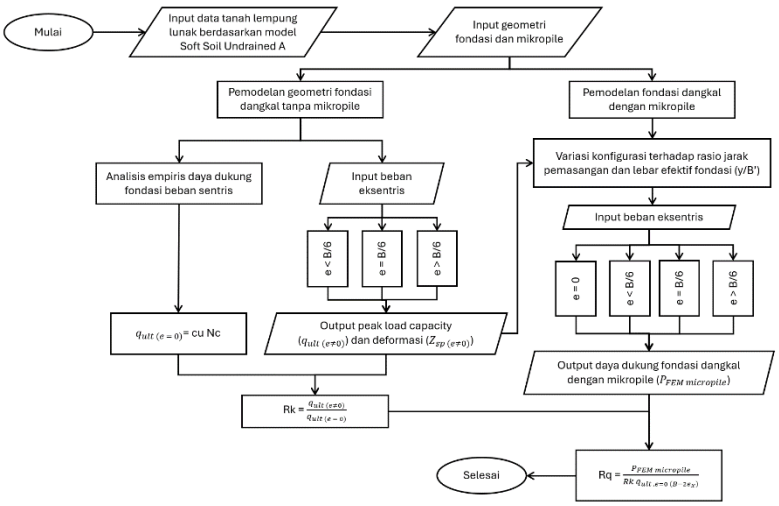

Figure 4. Flowchart of Numerical Analysis for Shallow Foundation Modeling with and without Micropiles.

Both numerical analyses were modeled using a plane strain model. A triangular mesh element model with 15 nodes and a fine-to-medium size was used, as it provides good stress response quality and is well-calibrated to empirical approaches (Al-Dawoodi et al., 2022). This model interprets the shape of a continuous foundation (strip footing), where the shape factor (sc) is 1 (Sieffert & Bay-Gress, 2000). The width of the foundation (B) applied in the model is 1 meter. The foundation is assumed to be rigid

and rough. A fully fixed boundary condition will be applied to the bottom of the soil geometry, and a normally fixed boundary condition will be applied to both lateral sides of the soil geometry. Furthermore, undrained conditions are applied with a closed groundwater flow boundary condition.

There are two outcomes from the model under eccentric loading that will be analyzed further: the maximum deformation boundary due to eccentric loading ($Z_{sp,e\neq0}$) and the maximum load capacity ($q_{FEM,e\neq0}$). The maximum deformation due to eccentric loading will influence the micropile installation length (Figure 5(a)), and the effective width due to eccentricity will affect the micropile location (Figure 5(b)). The variations in micropile installation are summarized in Table 2, where micropiles are specifically installed in an unconnected condition to the foundation (unconnected pile). A 0.1-meter thick compacted sand layer with shear strength parameters, including cohesion (c') of 1 kPa, internal friction angle (ϕ') of 32°, and dry unit weight (γsat) of 18.55 kN/m³, is applied for the unconnected pile model.

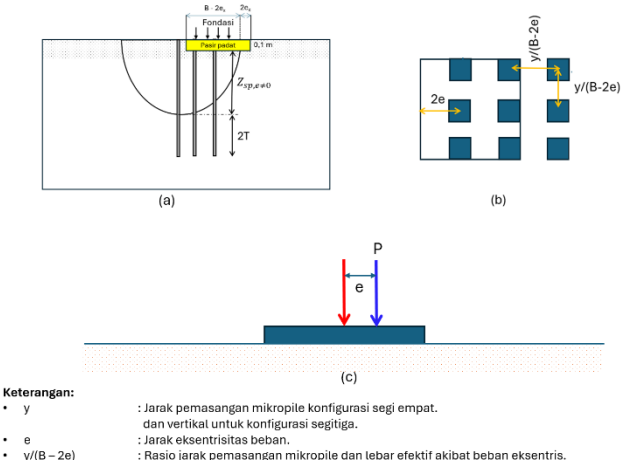

Figure 5. Definition of Shallow Foundation Model Configuration with Micropiles.

In addition, both the foundation and micropiles are designed with the same quality, specifically a compressive concrete strength (fc') of 42 MPa and an average unit weight of 24 kN/m³. Concrete is considered to fully contribute to the strength of the foundation and micropile material, so the elastic modulus representing both materials is 30,459,481.28 kPa. Additionally, the specific dimensions of the micropiles used are square cross-sectioned with a dimension (s) of 0.3 meters.

Table 2. Variations of Square Micropile Configuration.

y/B'	e (m)	B' (m)	Npile		
			4	9	16
			y (m)		
0,6	0	1,00	0,600		
0,6	0,1	0,80	0,480		
0,6	0,17	0,66	0,396		
0,6	0,25	0,50	0,300		
1,0	0	1,00	1,000		
1,0	0,1	0,80	0,800		
1,0	0,17	0,66	0,667		
1,0	0,25	0,50	0,500		

Sub 3 Perumusan Persamaan Daya Dukung Fondasi Akibat Perkuatan Micropile

The increase in soil bearing capacity is proposed from the development of formulations in previous studies (Isnaniati et al., 2024; Mochtar & Mochtar, 2025; Yudiawati et al., 2019). The development of the formulation is based on the force diagram shown in Figure 6. According to this force diagram, the bearing capacity increase formulation is influenced by the frictional force on the pile, the end resistance force on the pile, and the stiffness generated by the individual micropile.

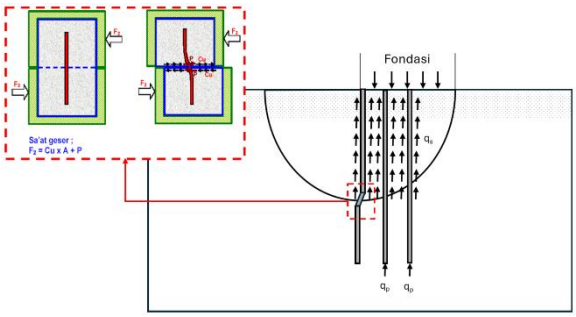

Figure 6. Force Diagram Due to Micropile Reinforcement.

The magnitude of the frictional force on the pile and the end resistance force are influenced by the number of piles (N), pile embedment depth (Ltotal), pile dimensions, and the shear strength of the soil. However, the resistance reactions from the pile tip and friction arise when the micropile is placed directly beneath the foundation. When the micropile is not placed under the foundation, the increase in bearing capacity is generated by the stiffness of the pile. The stiffness generated by the micropile can be determined by Equation 5 (Mochtar & Mochtar, 2025).

$$P_{\text{maks 1 pile}} = \frac{M_{\text{allow}}}{FM\ (T)} \tag{5}$$

The behavior of a single pile formulation should be composite (Figure 7) because it is modeled in two dimensions. Therefore, the allowable moment ($M_{allow\ pile}$) and the length affected by the allowable moment (T) should be influenced by the micropile configuration system. The composite value of T is calculated using Equation 6. Meanwhile, ($P_{maks,1\ pile}$) is determined from Equation 7.

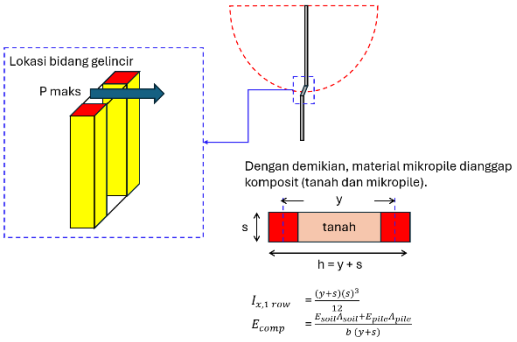

Figure 7. Micropile System as Composite Material.

Note: The elastic modulus of the soil (E_{soil}) for soft clay is 3500 kPa (Ameratunga et al., 2016).

$$T_{comp} = \left(\frac{E_{comp}\, I_{x\,1\,row}}{f}\right)^{0} \quad (6)$$

$$P_{maks\ 1\ row} = \frac{n_{pile\ 1\ row}}{FM\ (T_c} \quad (7)$$

Based on its configuration, the top view of the square configuration micropile as a composite material is shown in Figure 7. In addition to affecting the material stiffness, the frictional force generated by the soil and micropile will also be influenced. Therefore, the frictional force due to the micropile configuration is determined by the number of micropiles in a row (Equation 8). Based on Equation 8, the value of α is determined by the consistency of soft clay and micropile material, with α set to 1 (NAVFAC DM7.02, 1986).

$$Q_{s\ eq} = \alpha\ c_u\ A_{s\ eq} \quad (8)$$

Where:

- If $n_{micropile}$/row > 2, then $A_{s,eq} = s\ L_{total}\ (2n_{micropile} + 2)$,
- Otherwise, $A_{s,eq} = 2\ s\ L_{total}$

Based on the introduction to the schematic of concentric load distribution, the general equation (R_q) for the change in bearing capacity due to the addition of micropiles with the applied configuration system is presented in Equation 9. The force parameters resulting from the micropiles are neutralized with a function of the number of rows (n_{row}), cohesion (c_u), and the effective foundation area ($A' = B\ (B - 2\ e_x)$) in Equation9.

$$R_q = AX1 + BX2 + CX3 + D \quad (9)$$

Catatan:

- $X1 = \frac{\Sigma(n_{pile,1\ row}\ Q_p)}{n_{row}\ c_u\ A'}$
- $X2 = \frac{\Sigma\ Q_{s,eq}}{n_{row}\ c_u\ A'}$
- $X3 = \frac{\Sigma\frac{n_{pile,1\ row}\ (M_{allow\ 1\ pile})}{FM\ (T_{comp})}}{n_{row}\ c_u\ A'}$

Based on Equation 9, the proposed formulation has been modified from previous studies by (Isnaniati et al., 2024) by considering the forces and micropile configuration with the assumption of composite material (soil and micropile) for each row. The increase in bearing capacity (R_q) will be determined from the simulation results of the auxiliary program (P_{FEM}) and the empirical method ($Rk\ (q_{ult-empiris,e=0})(B - 2e_x)$). Meanwhile, a multi-variable regression method will be used to determine the coefficients (A), (B), (C), and the constant (D).

Results

Sub 1 Evaluation of Shallow Foundation Bearing Capacity Under Eccentric Load Without Micropiles

The bearing capacity of shallow foundations at the surface on soft clay soil with undrained cohesion (cu) of 14.95 kPa under concentric loading, using the

Terzaghi approach, yields values identical to the results of numerical analysis using the SS material model with fine to medium mesh sizes (Al-Dawoodi et al., 2022). Based on the empirical Terzaghi approach, the bearing capacity of the shallow foundation is as follows:

$$N_c = \frac{3\pi}{2} + 1 = 5{,}71$$

$$q_{ult,e=0} = c_u N_c$$

$$= 14{,}85\ (5{,}71) = 84{,}83\ kN/m^2$$

The results of the numerical analysis of the bearing capacity of the square foundation under eccentric loading on soft clay are presented in the load-deformation curve shown in Figure 9. Based on the curve in Figure 8, the bearing capacity of the foundation under each eccentric load on soft clay is summarized in Table 3. As shown in Figure 8, the soil deformation increases with the increasing eccentricity of the load. This is influenced by the increase in stress and forces at each node generated by the forces at the unbalanced point (e ≠ 0). The soil will reach failure at a certain deformation due to its inability to resist the total load or stress. Therefore, the bearing capacity is determined based on the maximum load occurring at the same deformation as the concentric load.

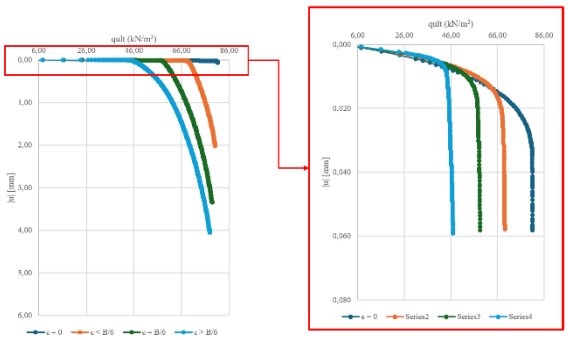

Figure 8. Load-Deformation Curve for Soft Clay Under Eccentric Load.

Table 3. Summary of Shallow Foundation Bearing Capacity on Soft Clay Without Micropiles Under Eccentric Load.

e/B	0	0,1	0,17	0,25
q_{ult}	84,83	69,30	58,73	47,20

Simulation results show that eccentricity reduces the foundation bearing capacity by up to 44% compared to concentric loading (Table 3). Based on the bearing capacity analysis of the foundation on soft soil under eccentric loading presented in Table 3, it can be seen that, in general, eccentric loading results in a downward trend in soft soil bearing capacity. The magnitude of the bearing capacity reduction due to eccentricity (e/B) is determined by the reduction factor (Rk), which is formulated in Equation 10. The results of these calculations are summarized in Table 4.

$$R_k = \frac{q_{ult,e\neq0}}{q_{ult,e=0}} \qquad (10)$$

Table 4. Summary of Bearing Capacity Reduction for Shallow Foundations Due to Eccentric Load.

e/B	R_k	$1 - R_k$
0,00	1,00	0,00
0,10	0,82	0,18
0,17	0,69	0,31
0,25	0,56	0,44

The relationship between the reduction factor (Rk) and eccentric load (e/B) is formulated in Equation 11 (Purkayastha & Char, 1977). In the linear regression function, the coefficient b will be equal to 1 in Equation 11. Furthermore, the regression function from the plot of (1 – R_k) values and the load eccentricity ratio (e/B) in Table 4 results in Equation 12, with a root square value approaching 1 and a coefficient a value of 1.7765 in Figure 9.

$$R_k = 1 - a\left(\frac{e}{B}\right)^b \tag{11}$$

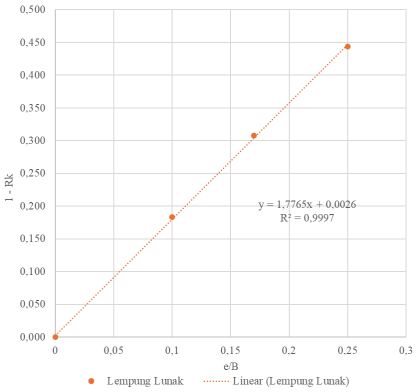

Figure 9. Regression Plot of Bearing Capacity Reduction for Shallow Foundations Due to Eccentric Load.

$$y(x) = 1 - R_k \tag{12}$$

$$R_k = 1{,}7765\ (e/B) - 0{,}9974 \tag{13}$$

Based on the bearing capacity reduction equation for shallow foundations under eccentric load on soft clay in Equation 13, the bearing capacity of shallow foundations under eccentric load can be formulated in Equation 14.

$$q_{ult,\ e\neq o} = 5{,}73\ c_u(1{,}781(e/B) - 1) \tag{14}$$

The numerical analysis results of the shallow foundation modeling under eccentric load show an asymmetric deformation shape, as presented in Figure 10. Eccentric load causes deeper deformation compared to concentric loading (e = 0). However, as the eccentricity of the load applied to the shallow foundation increases, the deformation depth does not increase significantly and tends to become identical. The average maximum deformation depth ($\overline{Z_{sp,e\neq0}}$) caused by eccentric load, as

summarized in Table 5, is 0.909 meters.

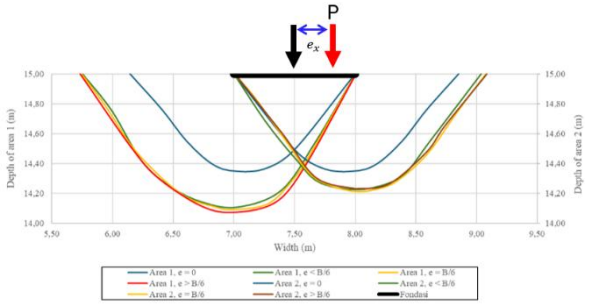

Figure 10. Deformation of Foundations on Soft Clay Due to Eccentric Load.

Table 5. Summary of Bearing Capacity Reduction for Shallow Foundations Due to Eccentric Load.

e/B	Z_{sp}(m)	$\lvert Z_{sp,e\neq0} - Z_{sp,e=0}\rvert$(m)
0,00	0,651	0,000
0,10	0,894	0,243
0,17	0,907	0,256
0,25	0,927	0,276

Sub 2 Numerical Analysis of Bearing Capacity for Shallow Foundations Reinforced with Micropiles

The micropile embedment depth (L_{total}) is determined from the depth of foundation failure in soft clay due to eccentric load and twice the stiffness of the micropile, as shown in Equation 15 (Mochtar & Mochtar, 2025). Based on the previous numerical analysis for (Zsp) the calculation of the micropile embedment depth (L_{total}) is as follows:

$$L_{total} = \overline{Z_{sp,e\neq0}} + 2T \quad (15)$$

- E = 30495500 KPa
- s = 0,3 meter
- $I_x = \frac{1}{12}(0,3)^4 = 0,000675$ m⁴
- The value of f for soft clay with a cohesion of 14,85 KPa is 999,86 KN/m³ (Figure 11).
- $T = \left(\frac{EI}{f}\right)^{0,2} = \left(\frac{30495500\ (0,000675)}{999,86}\right)^{0,2} = 1,83$ meter
- $L_{total} = 0,909 + 2\ (1,83) = 4,57$ meter ≈ 5 meter

Based on the numerical analysis results and the analytical calculations performed, the micropile embedment depth (L_{total}) to be modeled is 5 meters. The micropile grade is determined based on the design compressive strength (fc'). Considering the micropile grade, the allowable stress (σ_{ijin}) of the micropile is assumed to be 25% of fc', so the value of σ_{ijin} is 10.500 KPa (SNI 2847:2019, 2019).

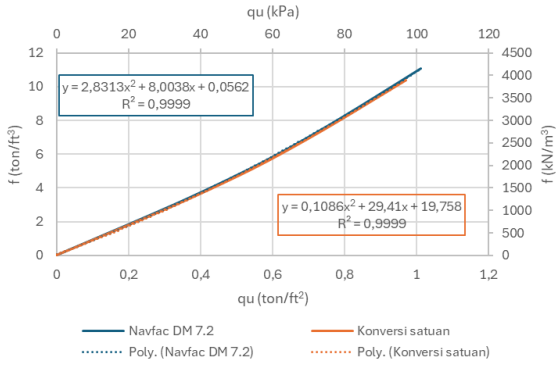

Figure 11. Relationship Between Coefficient of Subgrade Stiffness (f) and Maximum Soil Cohesion Stress (qu) (NAVFAC DM7.02, 1986).

Considering the allowable stress, the allowable moment of the micropile (M_{allow}) will be influenced by the section modulus, which is affected by the composite dimensions of the micropile. The relationship between the allowable moment of the micropile and the composite dimensions is formulated in Equation 16. Based on the composite system approach, the results of the numerical analysis for the square-configured micropile model are presented in Table 6.

$$M_{allow} = 10.500\ W_x(y) \tag{16}$$

Table 6. Summary of Bearing Capacity for Shallow Foundations with Square-Configured Micropiles Under Eccentric Load.

Configuration	P_{FEM} KN	$P_{ult,e\neq0}$ KN	R_q	X1	X2	X3
1	99,90	84,30	1,24	9,00	1,62	3,03
2	70,07	69,30	1,27	11,25	2,03	3,78
3	53,50	58,73	1,33	13,64	2,45	4,58
4	37,63	47,20	1,46	18,00	3,24	6,05
5	96,49	84,30	1,19	9,00	1,62	3,03
6	64,95	69,30	1,17	11,25	2,03	3,78
7	49,00	58,73	1,22	13,64	2,45	4,58
8	33,50	47,20	1,30	18,00	3,24	6,05
9	114,89	84,30	1,42	12,00	2,43	4,19
10	84,92	69,30	1,54	15,00	3,04	5,23
11	66,50	58,73	1,65	18,18	3,68	6,34
12	49,99	47,20	1,94	24,00	4,86	8,37
13	101,75	84,30	1,26	12,00	2,43	4,19
14	71,98	69,30	1,30	15,00	3,04	5,23
15	54,46	58,73	1,35	18,18	3,68	6,34
16	38,50	47,20	1,49	24,00	4,86	8,37
17	128,29	84,30	1,59	15,00	3,24	5,27
18	98,40	69,30	1,78	18,75	4,05	6,59
19	71,50	58,73	1,78	22,73	4,91	7,98
20	55,00	47,20	2,13	30,00	6,48	10,54
21	124,91	84,30	1,55	15,00	3,24	5,27

22	93,50	69,30	1,69	18,75	4,05	6,59
23	68,50	58,73	1,70	22,73	4,91	7,98
24	52,00	47,20	2,01	30,00	6,48	10,54

Based on the numerical analysis results presented in Table 6, values of Rq greater than 1 show a trend of increased bearing capacity for shallow foundations after being reinforced with micropiles compared to before reinforcement. The average increase in the bearing capacity of the shallow foundation after reinforcement with micropiles is 51.47%. However, the presence of eccentric load still leads to a reduction in the bearing capacity of the shallow foundation, even after reinforcement with micropiles. Based on the trend of bearing capacity changes (Rq), the correlation matrix results for variables X1 (0.869), X2 (0.905), and X3 (0.879) against R_q (Figure 12) show a very strong correlation using Pearson's analysis approach (Sugiyono, 2007).

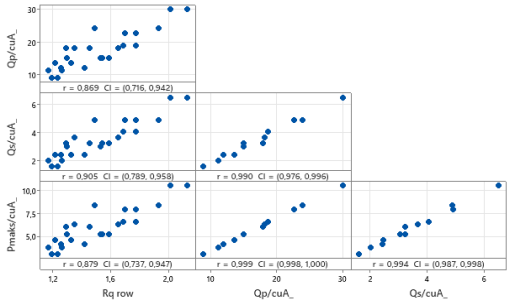

Figure 12. Correlation Matrix of Variables R_q, X1, X2, and X3 in Square Micropile Configuration, n = 24.

Sub 3 Bearing Capacity Formulation for Shallow Foundations Reinforced with Square-Configured Micropiles Under Eccentric Load

The results of the regression analysis with several formulation scenarios are presented in Table 7. Based on these scenarios, two formulations are identified with root square (R^2) values approaching 1. Therefore, further testing was conducted using the Analysis of Variance (ANOVA) approach. This test was performed to determine the significance of parameters X1, X2, and X3. The required critical value for the ANOVA analysis was obtained from the α value (0.05) and the F-value from the t-distribution probability values based on the Degree of Freedom (DF). The DF is formulated as n-1, where n is the number of observations (in this case, there are a total of 24 data observations), so DF is 23. Based on the DF value, the F-value from the t-distribution table is 1.714 (Montgomery, 2001).

Table 7. Summary of Formulation Scenarios for the Increase in Bearing Capacity of Shallow Foundations Due to Micropiles with Square Configuration.

Scenario	R^2	Variables		
		X1	X2	X3
1	81,80		V	
1	77,30			V
1	75,50	V		
2	85,50		V	V
2	85,30	V	V	

2	83,40	V		V
3	85,50	V	V	V

Based on the scenarios in Table 7, the R_q equation concerning variables X2 and X3 shows a significant relationship, as indicated by the F-value < F-value (11.87 for X2 and 5.28 for X3). The same is also shown by the P-value (0.002 for X2 and 0.032 for X3) < α (0.05). Based on the significance test using the ANOVA approach, the R_q formulation is derived from Equation 17.

$$R_q = 1{,}0259 + 0{,}538X2 - 0{,}233X3 \quad (17)$$

Conclusion

The results of the analysis conducted show that a decreasing trend in the bearing capacity of shallow foundations occurs due to the increase in eccentric loading. The same trend is observed even when micropiles have been simulated beneath the shallow foundation. However, the simulation evaluation results comparing the bearing capacity of the shallow foundation before and after the installation of square-configured micropiles show that the bearing capacity of the shallow foundation will increase by 51.47% compared to the condition before micropile installation. The assumption of micropiles and soil being considered as a composite material indicates that the micropile friction parameter (Qs or X2) and its stiffness (Pmaks or X3) play a significant role in formulating the increase in shallow foundation bearing capacity (Rq).

References

Agraine, H., Bouali, M. F., & Messameh, A. (2020). Numerical Analysis of One-Dimensional Consolidation in Fine-Grained Soils. *Key Engineering Materials*, *857*, 334–340. https://doi.org/https://doi.org/10.4028/www.scientific.net/KEM.857.334

Al-Dawoodi, B. A., Waheed, M. Q., & Rahil, F. H. (2022). Numerical Modeling of Shallow Foundation Behavior Using Soft Soil Model. *IOP Conference Series: Earth and Environmental Science*, *961*(1). https://doi.org/10.1088/1755-1315/961/1/012057

Alhassani, A. M. J., & Aljorany, A. N. (2019). Performance of piled raft foundation supported by either connected or unconnected piles. *IOP Conference Series: Materials Science and Engineering*, *584*(1). https://doi.org/10.1088/1757-899X/584/1/012045

Alnuaim, A. M., El Naggar, M. H., & El Naggar, H. (2016). Numerical investigation of the performance of micropiled rafts in sand. *Computers and Geotechnics*, *77*, 91–105. https://doi.org/https://doi.org/10.1016/j.compgeo.2016.04.002

Ambassa, Z., & Amba, J. C. (2020). Assessment of Stiffness and Strength Parameters for the Soft Soil Model of Clays of Cameroon. *Advances in Civil Engineering*, *2020*, 1–16. https://doi.org/10.1155/2020/8877367

Ameratunga, J., Sivakugan, N., & Das, B. M. (2016). *Correlations of Soil and Rock Properties in Geotechnical Engineering*.

Brinkgreve, R. B. J. (2012). Selection of Soil Models and Parameters for Geotechnical Engineering Application. *Soil Constitutive Models: Evaluation, Selection, and Calibration*, 69–98. https://doi.org/https://doi.org/10.1061/40771(169)4

Dhana Sree, N., Saibaba Reddy, E., & Padmavathi, V. (2022). Behavior of Single Pile Subjected to Eccentric Loading in Cohesionless Soils. *Lecture Notes in Civil*

Engineering, *167*, 591–603. https://doi.org/10.1007/978-981-16-3383-6_52
Doherty, J., Alguire, H., & Wood, D. M. (2012). Evaluating modified Cam clay parameters from undrained triaxial compression data using targeted optimization. *Canadian Geotechnical Journal*, *1292*, 1285–1292. https://doi.org/10.1139/t2012-088
Eastwood, W. (1955). The Bearing Capacity of Eccentrically Loaded Foundations on Sandy Soils. *The Structural Engineer*, *3*, 181–187.
Franza, A., & Sheil, B. (2021). Pile groups under vertical and inclined eccentric loads: Elastoplastic modelling for performance based design. *Computers and Geotechnics*, *135*. https://doi.org/10.1016/j.compgeo.2021.104092
Isnaniati, & Mochtar, I. B. (2023). Increasing the Bearing Capacity of Shallow Foundations on Soft Soil After the Installation of Micro-Piles. *Journal of the Civil Engineering Forum*, *9*(September), 227–238. https://doi.org/10.22146/jcef.5925
Isnaniati, Mochtar, I. B., & Mochtar, N. E. (2024). Study of Changes in the Ultimate Bearing Capacity Shallow Foundations in Soft to Medium Consistency Clay Soils After Reinforcing Micro-Piles. *Advances in Civil Engineering Materials*, 669–682.
Kenya Engineer. (2017). *Foundation Failure Due to Column Eccentric Values*. 26–28.
Li, L., Zhou, P., Li, J., Miraei, S., Feng, P., & Wei, M. (2025). Pile installation effects in natural soft clays : A semi-analytical solution using strain path method. *Journal of Rock Mechanics and Geotechnical Engineering*, 1–17. https://doi.org/10.1016/j.jrmge.2025.01.003
Meyerhof, G. . (1953). The Bearing Capacity of Foundations under Eccentricand Inclined Loads. *International Society for Soil Mechanics and Geotechnical Engineering* , 440–445.
Michalowski, R. L., & You, L. (1998). Effective width rule in calculations of bearing capacity of shallow footings. *Computers and Geotechnics*, *23*(4), 237–253. https://doi.org/10.1016/S0266-352X(98)00024-X
Mochtar, I. B., & Mochtar, N. E. (2025). *Perkuatan Cerucuk untuk Fondasi Dangkal pada Tanah Lunak*. Deepublish.
Mohd, K., Saquib, N., & Showkat, R. (2018). Soil Constitutive Models and Their Application in Geotechnical Engineering : A Review. *International Journal of Engineering and Research & Technology (IJERT)*, *7*(04), 137–145.
Montgomery, D. C. (2001). *Design and Analysis of Experiments* (5th ed.). John Wiley & Sons, Inc.
NAVFAC DM7.02. (1986). Soil Mechanics Design Manual. In *Naval Facilities Enginering Command* (2nd ed., Vol. 36, Issue 4). Office, Washington, D.C.
Okamura, M., Mihara, A., Takemura, J., & Kuwano, J. (2002). Effects of Footing Size and Aspect Ratio on the Bearing Capacity of Sand Subjected to Eccentric Loading. *Soils and Foundations*, *42*(4), 43–56. https://doi.org/https://doi.org/10.3208/sandf.42.4_43
Plaxis 2D 2025.1. (2025). Material Models Manual. In *Seequent 2025* (2025.1). The Bentley Subsurface Company.
Prakash, R., & Rahul, N. (2020). *Comparative Analysis of Eccentrically Loaded Footing Using SAP2000- A Literature Review*. *8*(9), 119–123.
Prakash, S., & Saran, S. (1971). Bearing Capacity of Eccentrically Loaded Footings. *Journal of the Soil Mechanics and Foundations Division*, *97*(1), 95–117. https://doi.org/10.1061/JSFEAQ.0001544
Purkayastha, R. D., & Char, R. A. N. (1977). Stability Analysis for Eccentrically Loaded Footings. *Journal of the Geotechnical Engineering Division*, *103*(6), 647–651. https://doi.org/10.1061/AJGEB6.0000441
Seongcheol, H., Garam, K., Incheol, K., Qaisar, A., & Junhwan, L. (2021). Experimental and Numerical Studies on Load-Carrying Capacities of Encased Micropiles with Perforated Configuration under Axial and Lateral Loadings. *International Journal of Geomechanics*, *21*(6), 4021083. https://doi.org/10.1061/(ASCE)GM.1943-5622.0002019

Sieffert, J. G., & Bay-Gress, C. (2000). Comparison of European bearing capacity calculation methods for shallow foundations. *Proceedings of the Institution of Civil Engineers: Geotechnical Engineering*, *143*(2), 65–74. https://doi.org/10.1680/geng.2000.143.2.65

SNI 2847:2019. (2019). *Persyaratan Beton Struktural untuk Bangunan Gedung* (Issue 8). Badan Standardisasi Nasional.

Sugiyono. (2007). *Statistika Untuk Penelitian*. Ikatan Penerbit Indonesia (IKAPI).

Suroso, Harimurti, H., & Harsono, M. (2012). Alternatif Perkuatan Tanah Lempung Lunak (Soft Clay), Menggunakan Cerucuk Dengan Variasi Panjang dan Diameter Cerucuk. *Rekayasa Sipil*, *2*(1), 47–62.

Suroso, Munawir, A., & Indrawahyuni, H. (2010). Pengaruh Penggunaan Cerucuk dan Anyaman Bambu pada Daya Dukung Tanah Lempung Lunak. *Journal of Civil Engineering*, *4*(3), 161–174.

Terzaghi, K. (1943). Theoretical Soil Mechanics. In *Géotechnique*. Harvard Univercity. https://doi.org/10.1680/geot.1963.13.4.267

Tjandrawibawa, S. (2000). Peningkatan Daya Dukung Pondasi Dangkal Dengan Menggunakan Cerucuk Suatu Studi Model. *Civil Engineering Dimension*, *2*(2), 92–95.

Tsukada, Y., Miura, K., Tsubokawa, Y., Otani, Y., & You, G.-L. (2006). Mechanism of Bearing Capacity of Spread Footings Reinforced with Micropiles. *Soils and Foundations*, *46*, 367–376. https://doi.org/10.3208/sandf.46.367

Waheed, M. Q., & Asmael, N. M. (2024). Using soft soil models engineering : a review paper in geotechnical. *Ural Environmental Science Forum "Sustainable Development of Industrial Region"*, *531*, 1–8. https://doi.org/doi.org/10.1051/e3sconf/202453104018

Waheed, M. Q., & Rahil, F. (2022). Numerical Modeling of Shallow Foundation Behavior Using Soft Soil Model Numerical Modeling of Shallow Foundation Behavior Using Soft Soil Model. *2nd International Conference of Al-Esraa University College for Engineering Sciences*, *961*, 1–11. https://doi.org/10.1088/1755-1315/961/1/012057

Wang, J., Sun, G., Chen, G., & Yang, X. (2021). Finite element analyses of improved lateral performance of monopile when combined with bucket foundation for offshore wind turbines. *Applied Ocean Research*, *111*, 102647. https://doi.org/https://doi.org/10.1016/j.apor.2021.102647

Yudiawati, Y., Mochtar, I. B., & Mochtar, N. E. (2019). Group capacity and efficiency of full friction piles on very soft soil. *International Journal of GEOMATE*, *16*(57), 201–208. https://doi.org/10.21660/2019.57.68950.